Regional Studies in Marine Science 91 (2025) 104528

Contents lists available at ScienceDirect

Regional Studies in Marine Science

journal homepage: www.elsevier.com/locate/rsma

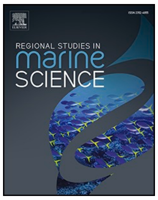

Factors influencing the early growth and dispersal potential of mangrove propagules

G. Thompson-Saud[a,c,*], A.I. Robertson[b], S. Choukroun[c], A. Ospina-Alvarez[d], M. Logan[e], M. van der Mheen[b], A. Grech[a]

[a] *College of Science and Engineering, James Cook University, Townsville, Queensland, Australia*
[b] *UWA Oceans Institute and School of Biological Sciences, University of Western Australia, Crawley, WA 6009, Australia*
[c] *The Centre of Tropical Water and Aquatic Ecosystem Research (TropWATER), Townsville, Queensland, Australia*
[d] *Mediterranean Institute for Advanced Studies, IMEDEA, CSIC-UIB, Carrer Miquel Marquès, 21, Esporles, Illes Balears 07190, Spain*
[e] *Australian Institute of Marine Science, PMB 3, Townsville MC, Townsville, QLD 4810, Australia*

ARTICLE INFO

Keywords:
Mangrove propagules
Dispersion
Propagules traits
Conservation
Management
Salinity
Buoyancy

ABSTRACT

Mangrove dispersal, characterised by propagule movement across complex coastal habitats, is essential for maintaining genetic diversity and ecological resilience. A comprehensive understanding of these processes requires information on the influence of mangrove propagule traits on dispersal potential. However, relatively few studies have investigated the behaviour of propagules in the water column, particularly their responses to different salinities and the duration of their buoyancy. The goal of this study is to enhance the understanding of mangrove dispersal potential by using an experimental approach to assess buoyancy and morphological attributes of 13 mangrove species in the central Great Barrier Reef (GBR) region of Queensland, Australia. Over 90 days, we measured the buoyancy of mangrove propagules and recorded changes in root and stem growth under different salinity conditions, tracking the progression of these traits over time. We found evidence for interspecies variation in buoyancy and diverse responses to salinity treatments, with propagule positioning in the water column changing over time. Most of the species showed potential for long-distance dispersal as they stayed afloat for part or most of the experiment. Additionally, we developed species-specific parameters and implemented them in biophysical models to assess mangroves dispersal trajectories. Our findings highlight the importance of integrating mangrove propagule traits in dispersal modelling given the variability in buoyancy behaviours observed among different species and their influence on dispersal and connectivity.

1. Introduction

Seed dispersal is a fundamental ecological process for the survival, reproduction and spatial distribution of plant communities (Howe and Miriti, 2004; Howe and Smallwood, 1982; Schupp et al., 2010). It supports genetic diversity, colonization of new habitats and ecological resilience to environmental and anthropogenic change. For many coastal and marine plants, dispersal mechanisms are intricately linked to water movement. Mangroves, which play a vital role in coastal ecology, climate regulation and human livelihoods, rely on the oceanic dispersal of their propagules to maintain genetic diversity and ecological stability across different habitats (Balbar and Metaxas, 2019; Cowen et al., 2007; Steinberg et al., 2016; Van der Stocken, Wee, et al., 2019). This dispersal may be influenced by coastal ocean, tidal and wind and wave dynamics, all of which can interact differently with propagules depending on their position in the water column. Understanding these potential dispersal pathways requires information on mangrove propagule traits, such as post-detachment viability, positive buoyancy duration and position of the propagule within the water column. This knowledge is crucial for effective mangrove population management and conservation, offering insights into their resilience and adaptive strategies in the face of environmental change.

Mangroves inhabit the coastal intertidal zones of tropical and subtropical regions, which are characterised by dynamic environmental conditions driven by tidal cycles, extreme weather and varying salinity levels (Duke et al., 1998). The reproductive seasons generally occur during the warmer months when conditions are favourable for seed germination and establishment (Tomlinson, 2016). Mangroves produce

---

[*] Corresponding author at: College of Science and Engineering, James Cook University, Townsville, Queensland, Australia.
E-mail address: gabriela.thompsonsaud@my.jcu.edu.au (G. Thompson-Saud).

https://doi.org/10.1016/j.rsma.2025.104528
Received 18 April 2025; Received in revised form 15 September 2025; Accepted 29 September 2025

flowers that undergo pollination by insects, birds, mammals or wind. Depending on the mangrove type, the seed may either remain attached to the tree until it germinates into a propagule (viviparous and crypto viviparous) or germinate independently from the parental tree (non--viviparous) (Tomlinson and Cox, 2000). Following detachment, the propagule may settle near the parental tree or travel on a passive journey covering small (e.g. within estuary or bays) or extensive distances (e.g. transoceanic) before reaching a suitable location to settle (Robertson and Alongi, 1995; Sousa et al., 2007; Van der Stocken, Carroll, et al., 2019). Long-distance dispersal in mangroves is facilitated by positive buoyant propagules that remain afloat for extended periods (e.g. *Xylocarpus granatum, Rhizophora stylosa* and *Ceriops tagal*), drifting with ocean surface currents, winds and waves, until reaching an appropriate settling location or becoming non-viable (Van der Stocken, Carroll, et al., 2019).

Salinity and the exposure time to ocean water can influence buoyancy, dispersal and survival of mangrove propagules (Clarke et al., 2001; Rabinowitz, 1978; Tonné et al., 2017). For instance, higher salinity increases water density, which may enhance propagule buoyancy and potentially extend dispersal distances. However, mangrove propagules can also undergo physiological changes influenced by salinity, such as water uptake and tissue softening (Aziz and Khan, 2001; Smith and Snedaker, 1995), which can further affect their buoyancy and floating orientation. For example, lower salinities may increase water intake, making propagules heavier and reducing positive buoyancy. Since propagules are exposed to varying salinity levels during dispersal, species with broader salinity tolerance are more likely to establish in a wider range of habitats. Previous work by Clarke et al. (2001) demonstrated interspecific variation in buoyancy and in some species, in response to salinity concentration. However, these experiments were limited to 15 days, a duration likely too short to capture the full dispersal window. While some studies suggest that mangrove propagules can stay afloat, on average, for approximately 75 days (Van der Stocken, Carroll, et al., 2019), no study to date has examined the duration of a broad range of mangrove species can stay alive and positive buoyant over extended periods.

Information on the survival, buoyancy and aerodynamics of mangrove propagules are crucial for the development of biophysical models of mangrove dispersal. Biophysical models of mangroves integrate biological information with hydrodynamic models to predict dispersal pathways of propagules and habitat connectivity (Di Nitto et al., 2013; Gouvêa et al., 2023; Hamilton et al., 2017; Ngeve et al., 2016; Proisy et al., 2016; Van der Stocken, Carroll, et al., 2019; Van der Stocken and Menemenlis, 2017; Zainol et al., 2022). While the utilization of biophysical models has significantly enhanced our understanding of mangrove dispersal, there is an urgent need to develop more robust biological parameters to better inform biophysical models. Information such as propagule morphology and buoyancy properties (Van der Stocken et al., 2015) is critical because these factors directly influence parameters like windage (the aerodynamic effect of wind on the exposed portion of the propagule, e.g. Breivik et al. 2011) and drift factor (the effect of wind-driven drift current on the submerged portion, e.g. Wu 1983), alongside the assessment of salinity concentration across various species to understand their capacity for dispersal and to determine the duration each species remains afloat while still alive.

The goal of our study is to enhance the understanding of mangrove dispersal potential by measuring a series of propagule traits in 13 mangrove species from the central Great Barrier Reef (GBR) region of Queensland, Australia. Specifically, we aimed to: (1) assess the impact of salinity and time on propagule positive buoyancy; (2) evaluate root and stem development as key components influencing viability and dispersal; and (3) compute species-specific factors (drift factor and windage) to inform mangrove dispersal modelling. Through an experimental approach, our study elucidated the complex interactions among time, salinity and morphological traits affecting mangrove propagule dispersal and identified which species possess the ability to float for an extended time and therefore have the potential for long-distance dispersal. These findings provide valuable insights into the factors driving mangrove dispersal dynamics in the GBR region and can inform studies in other regions, given the comprehensive assessment of mangrove propagule morphologies evaluated here.

2. Methods

2.1. Study area

The Great Barrier Reef (GBR) region of Queensland, Australia (Fig. 1) is a globally significant marine ecosystem, renowned for its rich biodiversity and complex habitats. The tropical climate, characterized by distinct wet and dry seasons, drives fluctuations in salinity levels. During the wet season, heavy rainfall and freshwater inflows from rivers can reduce salinity levels to as low as 15 PSU (Van Woesik, 1992), particularly near river mouths. In contrast, the dry season is associated with limited freshwater input and high evaporation rates, which can raise salinity levels to 37 PSU (Andutta et al., 2011). This range is relatively large when compared to typical open ocean salinity, which remains around 33–37 PSU (NASA, 2025).

The tidal ranges in this area are substantial, typically ranging from around 2–7 m, and play a critical role in the ecological dynamics and connectivity of reef habitats (Steinberg, 2007). The mangroves of the GBR extend along most of the 2300 km long coastline, hosting a rich variety of 41 species, covering an estimated area of approximately 1240 km^2 (Duke, 2006). This diversity represents 50 % of the world's mangrove species and the GBR region is among the healthiest mangrove ecosystems (Goudkamp and Chin, 2006). Mangroves perform important ecological functions in the GBR, including protecting the coastline from erosion, sequestering carbon, providing habitat to invertebrates like crustaceans, molluscs and insects, as well as supporting various vertebrates including juvenile fish, mammals, reptiles and birds (Kathiresan and Bingham, 2001). Mangroves in the GBR are exposed to threatening anthropogenic processes, including land-based pressures associated with coastal development, hydrology alterations and poor water quality. Natural disturbances such as storms, cyclones, heat waves and pest invasions have further contributed to some changes in mangrove condition (Duke et al., 2003; Houston, 1999; McKillup and McKillup, 1997). Over the past four decades, the distribution of mangroves in the GBR has undergone alterations, with expansions in certain areas and contractions in others (Chamberlain et al., 2020; Duke et al., 2003; Hamylton et al., 2023) resulting in no net change in the distributional area of mangroves. Mangroves are protected under the *Queensland Fisheries Act* 1994, Fish Habitat Area and Marine Park regulations, which prohibit the removal or harm of mangrove without a permit.

2.2. Field collection

During our study conducted in the central GBR, we collected propagules from 13 different mangrove species (Table 1). Each species was represented with 15 samples, obtained from six locations: Cape Cleveland (19°S, 147°E); Ross River, Rowes Bay and Bohle River in Townsville (19°S, 146°E); and Lucinda and Herbert River (18°S, 146°E; Fig. 1). The propagules were collected from different locations because the species are distributed across various coastal areas. This approach covered a variety of species, each characterized by distinct morphologies, buoyancy traits and dispersal capacities (Table 1). Propagules were selected based on visible maturity (fully developed and firm), size range appropriate for the species and absence of physical damage or disease. To maintain the condition of the propagules, mature specimens were harvested directly from the trees to prevent prolonged contact with saltwater, thereby minimizing the risk of altering osmotic processes before the experiments. It is noteworthy that *Heritiera littoralis*, the only exception to this practice, was sourced from the soil surrounding the parental tree, as no specimens where found attached to the trees.

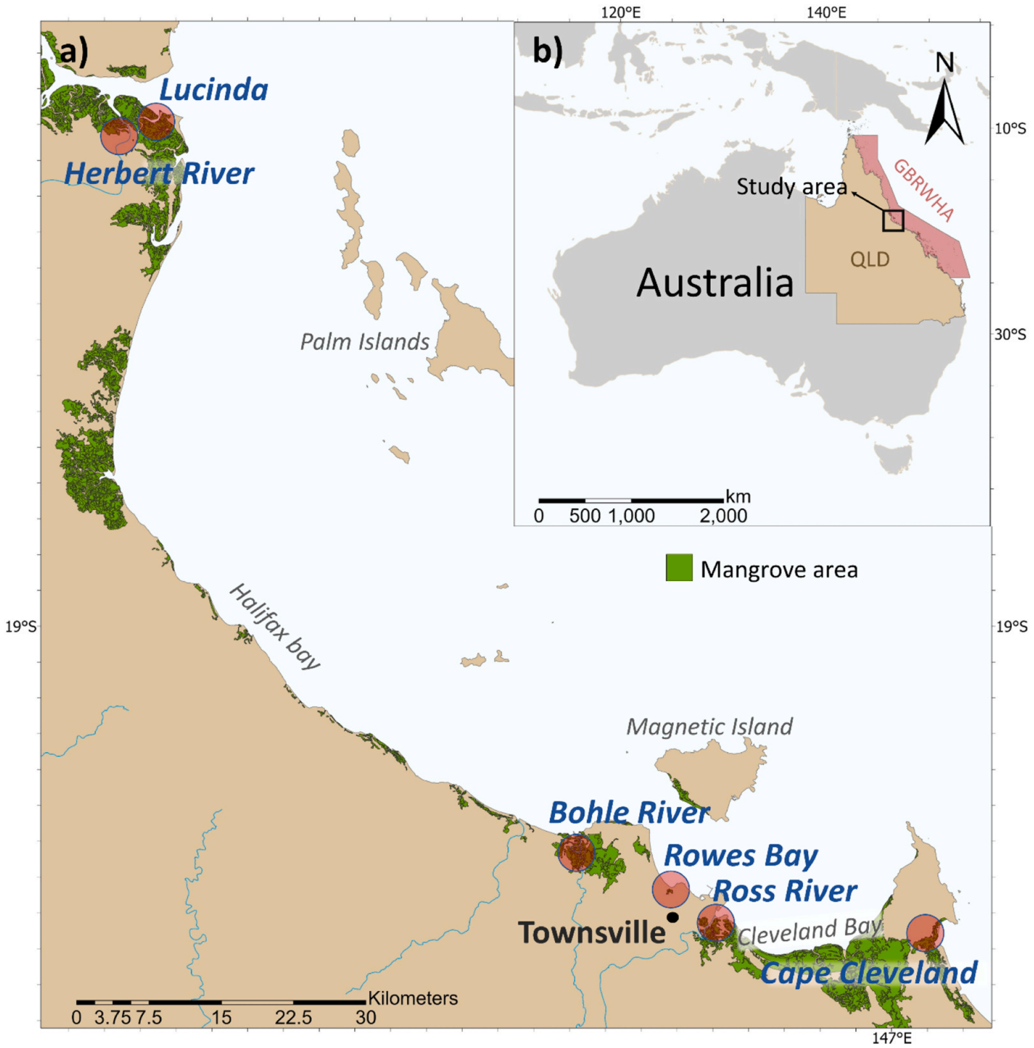

Fig. 1. a) Mangroves' geographic distribution in the study area. Areas coloured green are mangrove habitats and light blue lines are rivers. The red circles and their corresponding names in blue are the locations where propagules were collected. b) Map of Australia, with Queensland (QLD) coloured brown and the Great Barrier Reef World Heritage Area (GBRWHA) shown in red. The study area is indicated by a black square.

Table 1

General information about the mangrove species collected and the area from which they were collected. Vivipary refers to the method of seed germination specific to mangroves where the seed begins to develop while still attached to the parental tree; germination describes whether the seed germinates above (epigeal) or below (hypogeal) the ground; and the dates are formatted as DD/MM/YYYY.

Species	Family	Vivipary	Propagule type	Germination	Area collected	Intertidal position	Date of collection
Nypa fruticans	Arecaceae	Crypto viviparous	Seed	Epigeal	Herbert River	Low	12/01/2023
Bruguiera gymnorhiza	Rhizophoraceae	Viviparous	Seedling	Epigeal	Lucinda	High	26/01/2023, 8/03/2023
Xylocarpus granatum	Meliaceae	Non-viviparous	Seed	Hypogeal	Lucinda	High	26/01/2023
Ceriops australis	Rhizophoraceae	Viviparous	Seedling	Epigeal	Lucinda	Mid	26/01/2023
Ceriops tagal	Rhizophoraceae	Viviparous	Seedling	Epigeal	Lucinda	Mid	26/01/2023
Lumnitzera racemosa	Combretaceae	Non-viviparous	One-seeded fruit	Epigeal	Bohle River		8/02/2023
Rhizophora stylosa	Rhizophoraceae	Viviparous	Seedling	Epigeal	Ross River and Lucinda	Low and mid	30/01/2023, 8/03/2023
Heritiera littoralis	Malvaceae	Non-viviparous	One-seeded fruit	Hypogeal	Lucinda	High	8/02/2023
Bruguiera exaristata	Rhizophoraceae	Viviparous	Seedling	Epigeal	Cape Cleveland	High	8/02/2023
Avicennia marina	Acanthaceae	Crypto viviparous	Seed	Epigeal	Rowes Bay	Low	10/02/2023
Sonneratia alba	Lythraceae	Non-viviparous	One-seeded fruit	Epigeal	Rowes Bay	Low	8/02/2023, 10/02/2023
Excoecaria agallocha	Euphorbiaceae	Non-viviparous	One-seeded fruit	Epigeal	Cape Cleveland	High	30/01/2023
Aegialitis annulata	Plumbaginaceae	Crypto viviparous	One-seeded fruit	Epigeal	Rowes Bay	Mid	29/03/2023

Due to the inherent difficulty in ascertaining the duration these propagules spent on the soil and in contact with saltwater before collection, we excluded this species from the statistical analyses to prevent potential bias. To ensure uniformity in our measurement procedures, all propagules underwent assessment (measuring length, width, weight, etc.) on the day immediately following their collection.

2.3. Laboratory-based assessment of propagule dynamics

The experiment involved placing propagules in water tanks with varying salinity levels of 35, 22.5 and 10 practical salinity units (PSU) for a total of 90 days. These salinity levels likely represent conditions that propagules might encounter as they move through different environments, from estuarine areas to open ocean waters with varying freshwater input. Each tank contained five propagules of a single species, constituting three distinct treatment groups for each species. The tanks were situated in the Marine and Aquaculture Research Facility (MARFU) laboratory at James Cook University, Townsville, where a constant temperature of 25°C was maintained using an air conditioner. To ensure uniform conditions, the water in the tanks underwent stirring every three days, with salinity measurements taken at five-day intervals. Additional freshwater was introduced as needed to compensate for changes in salinity concentrations resulting from evaporation. Propagules were measured daily for the initial five days and subsequently at five-day intervals until day 90. The comprehensive set of measurements included weight, length, width, buoyancy (considering both overall buoyancy and the specific length of the portion of the propagule outside the water), orientation, as well as root and stem initiation, length and quantity. This detailed monitoring approach aimed to capture the changing physical characteristics of the propagules throughout the 90-day experimental period.

2.4. Data analysis

Bayesian hierarchical models were used to examine two aspects of mangrove propagule buoyancy in response to salinity over time: (1) propensity of propagules to float and (2) percentage of propagule above the water surface. To determine the percentage above water, the portion of each propagule protruding above and below the waterline was measured using a ruler. This measurement was taken in a two-dimensional manner, reflecting the linear distance above and below water. Each model was fitted separately for each of the 13 mangrove species and included population effects of salinity (levels: 35, 22.5 and 10 PSU), time (1–90 days) and their interactions. Models also included the varying effect of propagule ID to account for the dependency structure introduced by repeated measurements of the same sampling units. In the buoyancy propensity, time was scaled (mean: 0, standard deviation (sd): 1) to assist model convergence.

All models employed weakly informative priors across all parameters (Table A.1). More specifically, normal priors were used for the intercept and all population effects, while half student t-distributions (3 degrees of freedom (df)) were applied to the varying (sd) parameters. Where required, priors on shape parameters were based on gamma distributions.

All models were fit using the R “brms” package (Bürkner, 2017) within the R Statistical and Graphical Environment (R Code Team, 2019) and included a total of 5000 iterations after a warmup of 1000, thinning to a rate of five across three chains. Markov chain Monte Carlo (MCMC) chain mixing and convergence were confirmed from a series of diagnostics (trace plots, autocorrelation plots, r-hat and effective sample size statistics). Model validations, including goodness of fit, heteroscedasticity and overdispersion, were performed using posterior predictive checks and simulated residuals (DHARMa) (Hartig, 2020). If there were multiple potential valid candidate models per species, leave-one-out information criterion (loo) (Yao et al., 2017) was used to select the best model.

The buoyancy propensity models (binary data) were fitted against a binomial (logit link) family (Eq. 1). Days 2, 3 and 4 were excluded prior to modelling as they did not provide additional information, and their exclusion helped to regularize the temporal covariate.

$$
\begin{aligned}
y_{ij} &\sim Bin(\pi_{ij}, 1) \\
\log\left(\frac{\pi_{ij}}{1-\pi_{ij}}\right) &= \beta_0 + \sum_{s=1}^{n} \beta_s S_i \, x \, \beta_t scale(T_i) + \gamma_j Z_i \\
\gamma_j &\sim N(0, \sigma_j) \\
\beta_j &\sim N(n, v) \\
\beta_{[1,n],t} &\sim N(0, v) \\
\sigma_j &\sim t(3, 0, v)
\end{aligned}
\tag{1}
$$

Flotation γ_{ij} of the j_{th} propagule at the i_{th} time point was assumed to be drawn from a binomial distribution parameterised by the probability of floating (π_{ij}). The (natural log of the odds of) probabilities were described by a linear model that included the varying effects of ID (γ_j) as well as an intercept (β_0) and the population effects ($\beta_{[1,n],t}$) of salinity (S_i) crossed with scaled time ($scale(T_i)$). Constants n and v above were calculated from the observed data.

The models for the percentage of propagule above water were fitted using a beta (logit link) family (Eq. 2). Instead of scaling the time covariate, it was transformed to a logarithmic scale and then rescaled to the range [0−1] to ensure that the model intercepts represented the expected percentage above water at the start of the experiment. This transformation was performed to maintain interpretability of the intercepts despite variations in the duration each propagule remained buoyant throughout the time series. The percentage of propagule above water was modelled for several species (*N. fruticans, B. gymnorhiza, X. granatum* and *S. alba*). Other species exhibited minimal variation across salinity and time, hindering model stability. Therefore, these species were excluded from these models.

$$
\begin{aligned}
y_{ij} &\sim beta(\mu_{ij}, \varnothing) \\
\log\left(\frac{\mu_{ij}}{1-\mu_{ij}}\right) &= \beta_0 + \sum_{s=1}^{n} \beta_s S_i \, x \, \beta_t scale(T_i) + \gamma_j Z_i \\
\varnothing &\sim T(0.01,\ 0.01) \\
\gamma_j &\sim N(0, \sigma_j) \\
\beta_0 &\sim N(n, v) \\
\beta_{[1,n],t} &\sim N(0, v) \\
\sigma_j &\sim t(3, 0, v)
\end{aligned}
\tag{2}
$$

For the bouyancy models, days at which the propagules are most likely to sink were calculated as -β_0/β_t (conditional on salinity level) from the full posteriors before being summarised to median and lower/upper highest probability density intervals (rounded to integer days).

Percentage above water (y) of the j_{th} propagule at the i_{th} time was assumed to be drawn from a beta distribution parameterised respectively by the probability of floating (π_{ij}) and a dispersion ($\varnothing$) parameter. The (natural log of the odds of) probabilities were described by a linear model that included the varying effects of ID (γ_j) as well as an intercept (β_0) and the population effects ($\beta_{[1,n],t}$) of salinity (S) crossed with rescaled logarithm transformed time (T). Constants n and v above were calculated from the observed data.

Once the models were run and validated, for each species, pairwise contrasts between each of the salinity levels were conducted across the posteriors marginalising over time. Evidence for differences was thereafter based on Bayesian exceedance probabilities. Finally, for the buoyancy models (binomial), days at which propagules are most likely to sink were calculated using LD50, which represents the time when 50 % of the seeds are expected to sink.

In addition to the statistical analyses, a quantitative metric was developed to account for root growth observed during the experiment. Specifically, a “root energy” index was calculated as the product of the number of roots and the length of the longest root, as defined in Eq. 3. This metric allowed for a simple comparative assessment of root development across species and salinity treatment. Among the species studied, only *B. gymnorhiza, X. granatum, C. australis, B. exaristata, A. marina* and *E. agallocha* developed roots at some point during the 90-day experiment (Fig. 3).

$$\textit{Root energy} = \textit{Root number} * \textit{Longest root} \tag{3}$$

2.5. Factors for species-specific mangrove modelling

A common approach to incorporate wind effects on propagules, such as seeds and fragments, in biophysical dispersal models is to add 3 % of the wind speed to the velocity of virtual particles (Tsanis, 1989). However, this approach may not always represent what happens, as the buoyancy of the propagules also influences the wind's effect. To address this, we developed a species-specific parametrization for Lagrangian particle tracking models to improve simulations of mangrove dispersal. Instead of using the standard 3 %, we calculated the drift factor ($\overrightarrow{u}_{drift}$) and windage ($\overrightarrow{u}_{windage}$). These parameters can be added to the current velocity ($\overrightarrow{u}_{current}$) to more accurately represent the wind's impact on propagule dispersal. Drift factor and windage were determined based on propagule morphology, specifically assessing the proportion submerged and exposed. The drift factor, representing the effect of the wind-driven drift current on the submerged portion of the propagule, was calculated using Eq. 4 (Van der Mheen et al., 2020). Windage, which accounts for the effect of wind on the exposed portion of the propagule, was calculated using Eq. 5.

$$\overrightarrow{u}_{drift} = \left[\alpha - \left(\frac{1}{k\sqrt{\frac{\rho_a + \quad C_d}{\rho_w}}}\right)\log\left(\frac{z}{z_0}\right)\right] * \quad \overrightarrow{u}_{10} \tag{4}$$

where α is 0.03, k is von Karman's constant (0.41), ρ_a is the air density (1.2 kg/m^3), ρ_w is the water density, which was approximated to 1025 kg/m^3 across all salinity treatments, given the relatively small variation in water density among them. C_d is the drag coefficient (0.00105 for wind speed under 7 m/s), z_0 is the roughness length of the ocean side (assumed to be a small non-zero value, -0.001 m) [37], z is the depth, representing the length of the propagule submerged in water and $\overrightarrow{u}_{10}$ is the wind speed at 10 m.

$$\overrightarrow{u}_{windage} = \sqrt{\frac{\rho_a \quad C_{Da} \quad A_a}{\rho_w \quad C_{Dw} \quad A_w}} * \quad \overrightarrow{u}_{10} \tag{5}$$

where ρ represents the fluid density, C_D is the drag coefficient of the object, A stands for the effective exposed area and the subscripts a and w denote the parameters on the air and water sides, respectively. $\frac{\rho_a}{\rho_w}$ is equal to $1.17 \cdot 10^{-3}$, $\frac{C_{Da}}{C_{Dw}}$ assumed to be equal to 1 (Isobe et al., 2011) and the $\frac{A_a}{A_w}$ is calculated for each species using the length of the propagule that is outside of the water, divided by the length that is inside the water. Although A represents the area, this ratio can be simplified by using lengths instead of areas because the proportional relationship holds true for both measurements since the propagules are approximately symmetrically shaped for most mangrove species.

To guide our determination of which species require consideration of salinity and time variations when calculating these factors, we employed the outputs of our statistical analysis, which assessed whether the percentage of propagules above the water surface was influenced by salinity and time. For species that developed roots and/or stem, we also considered the length of the longest root and the length of the stem. The only exception was *A. marina*, as their irregular shape and orientation made it difficult to identify what was above and what was below the waterline.

Once the parameters were calculated, we implemented them in test simulations for *Bruguiera gymnorhiza* and *Rhizophora stylosa* by adjusting propagule velocity as a function of hydrodynamic and wind velocities and applying graph theory to the resulting connectivity patterns with and without drift factor and windage. The detailed formulation and implementation of these parameters are provided in Appendix B.

3. Results

The morphological characteristics of mangrove propagules exhibited substantial variation across different species. Sizes and shapes ranged from small and rounded, like *Excoecaria agallocha*, to long and elongated, such as *Rhizophora stylosa* (Table 2). The orientation of the propagules in the water column also showed variability, influenced by the propagule shape and the time of measurement. For instance, elongated species like *Bruguiera gymnorhiza* predominantly maintained a vertical position, while other elongated species such as *Ceriops tagal, R. stylosa* and *Aegialitis annulata* were predominantly in a horizontal position (Fig. 2). However, certain species with elongated propagules, like *Ceriops australis* and *Bruguiera exaristata*, exhibited a similar amount of time spent in both vertical and horizontal positions. Across species, propagule length and width were positively associated with buoyancy duration, whereas heavier propagules tended to sink faster (Appendix C).

Root and stem development were observed in some propagules, including *B. exaristata, Xylocarpus granatum* and *Avicennia marina*. In contrast, other species, such as *Nypa fruticans, C. tagal, Lumnitzera racemose, R. stylosa, Heritiera littoralis* and *Sonneratia alba,* did not exhibit any development of roots or stems during the 90-day experimental period. Root initiation ranged from 26 to 82 days, while stem initiation occurred between 63 and 70 days across various species.

3.1. Propagule buoyancy

The 13 species exhibited diverse responses in buoyancy to the salinity treatment and time after detachment (Fig. 2 and Fig. C1). For instance, *A. marina* submerged during the early stages of the experiments but subsequently resurfaced after a few days (Fig. 2j). Conversely, species like *S. alba* and *A. annulata* sank initially and did not undergo refloating (Fig. 2k and m). Notably, propagules of *R. stylosa* sank only in the treatment with a salinity of 10 PSU, while those in the other treatments remained afloat (Fig. 2g). In the case of *S. alba*, one propagule in the 22.5 PSU salinity treatment exhibited a unique behaviour by opening on the second day releasing over 100 seeds. Initially buoyant, these seeds gradually started sinking on day five, with approximately half of them floating by day 90. Certain species either consistently exhibited minimal sinking throughout the study or sank most of their propagules in the initial days of experiments, making statistical measurement impractical due to limited observable changes. The buoyancy of *N. fruticans, L. racemose* and *E. agallocha* in relation to salinity and time was statistically tested. Importantly, once a propagule sank for the first time, it was considered to remain submerged, even if subsequent refloating occurred. This methodology was chosen both for statistical purposes and to align with the ecological realism of mangrove dispersal dynamics, where propagules are likely to become attached to the substrate after an initial sinking event.

The results of the statistical analyses conducted across all species indicate that there was evidence of differences in propagule positive buoyancy across all salinity concentrations. In general, propagules became less positively buoyant at lower salinity, with an 86 % decrease at 22.5 PSU and by 90 % decrease at 10 PSU compared to 35 PSU (Table A.2). This trend was consistently observed in *N. fruticans* and *E. agallocha*. However, *L. racemosa* exhibited a decline in positive buoyancy only between 10 and 35 PSU. Notably, positive buoyancy changed over time across all propagules. In addition, expected sinking times varied among species and salinity treatments, with each species displaying distinct patterns in the number of days before becoming

Table 2
Mangrove propagules characteristics, including mean mass, length, width, shape, predominant orientation, percentage of propagules that developed root and stem during the 90-day experiment and the average day that this happened.

Species	Mean weight (g)	Mean length (cm)	Mean width (cm)	Shape	Predominant orientation	Seeds that developed roots (%)	Day of root initiation	Seeds that developed stem (%)	Day of stem initiation
Nypa fruticans	42.56	6.98	4.41	Oblong ellipsoid	Horizontal	0	n/a	0	n/a
Bruguiera gymnorhiza	27.23	20.2	1.53	Cigar shaped	Vertical	93	58	93	66
Xylocarpus granatum	23.44	4.5	4.3	Angular and tetrahedral	Horizontal	93	30	27	63
Ceriops australis	2.01	13.65	0.59	Pencil like but tapered	Vertical	100	50	0	n/a
Ceriops tagal	6.3	19.69	0.92	Pencil like but tapered	Horizontal	0	n/a	0	n/a
Lumnitzera racemosa	0*	1.71	0.46	Oblong ellipsoid	Horizontal	0	n/a	0	n/a
Rhizophora stylosa	35.1	37.59	1.37	Elongated	Horizontal	0	n/a	0	n/a
Heritiera littoralis	19.11	5.24	3.35	Slightly flattened ellipsoidal	Horizontal	0	n/a	0	n/a
Bruguiera exaristata	4.26	11.73	0.84	Cigar shaped	Vertical	100	28	100	70
Avicennia marina	4.38	2.22	2.1	Rounded	Horizontal	100	26	100	69
Sonneratia alba	20.74	2.76**	2.76**	Sickle shaped	Vertical	0	n/a	0	n/a
Excoecaria agallocha	0*	0.4**	0.4**	Spherical	n/a	80	27	0	n/a
Aegialitis annulata	0.38	6.55	0.3	Elongated	Horizontal	67	82	0	n/a

* Imperceptible to the scale
** Diameter

negatively buoyant (Table A.3).

3.2. Percentage of propagule above the water surface

Overall, we found that, among the species tested, the proportion of the propagule remaining above the water surface declined more rapidly at lower salinities. Specifically, the decline was 51 % greater at 10 PSU than 35 PSU (Table A.4). This trend was consistent in *B. gymnorhiza*. However, *S. alba* showed a different pattern, with the decline being 85 % lower at 22.5 PSU compared to 35 PSU, indicating a slower loss of exposed surface area at intermediate salinity. Additionally, the proportion of the exposed area of the propagules varied over time for *N. fruticans, B. gymnorhiza* and *X. granatum*.

3.3. Root growth

'Root energy', defined as the product of the number of roots and the length of the longest root, was calculated for *B. gymnorhiza, X. granatum, C. australis, B. exaristata, A. marina* and *E. agallocha,* the only species that developed roots at some point during the 90-day experiment (Fig. 3).

Overall, root energy varied across species and salinity levels, with 10 PSU consistently having the highest root energy. In contrast, 22.5 PSU resulted in the lowest root energy across all species. Growth trends also differed among species. For instance, *B. gymnorhiza* and *X. granatum* exhibited a sharp increase in root energy after day 50, whereas *B. exaristata* displayed a more gradual and steady increase over time. Additionally, *X. granatum* and *A. marina* produced higher overall root energy compared to the other species that developed roots.

3.4. Factors for species-specific mangrove modelling

The calculated values for drift factor and windage, derived from assessments of propagule morphology, including the proportion submerged and exposed, are presented in Table 3. We obtained values for drift factor and windage for each species and incorporated different salinities and time when appropriate. It is important to note that for some species, windage might not be suitable to include in the model. Even if the proportion above the waterline is high, if the length is negligible, the effect of the drift current is likely more significant than windage, which acts directly on the area of the object that protrudes from the water surface.

Implementing drift factor and windage revealed species-specific differences in propagule dispersal and resulted in distinct patterns compared to models without these factors (Table 4). For *R. stylosa*, including the drift factor slightly increased short-term dispersal but reduced long-term distances (median distance: 5.9 m at day one and 411.4 m at day 90) compared to the model without drift (4 m at day one and 730.3 m at day 90). It also promoted northward dispersal (61.8 % of particles vs. 24.6 % without drift) and overall connectivity, nearly doubling the number of edges, increasing network density and halving the number of clusters, although modularity was slightly lower. Network diameter and the number of connected components remained unchanged, indicating that overall network structure was maintained. For *B. gymnorhiza*, adding drift factor and windage produced similar early dispersal but shorter long-term distances (7.3 m with drift factor and windage vs 7.7 m without at day one and 425.2 m with vs. 865.8 m without at day 90) and shifted the main dispersal direction southward (49.2 % of particles vs. 44.5 % northward without these factors) and slightly reduced connectivity, with fewer edges, lower network density and less cohesive clusters, while network diameter and connected components remained unchanged. Models without windage formed more clusters with higher modularity, reflecting stronger internal community structure.

4. Discussion

The findings of this study reveal substantial variability among different species of mangrove propagules in terms of buoyancy,

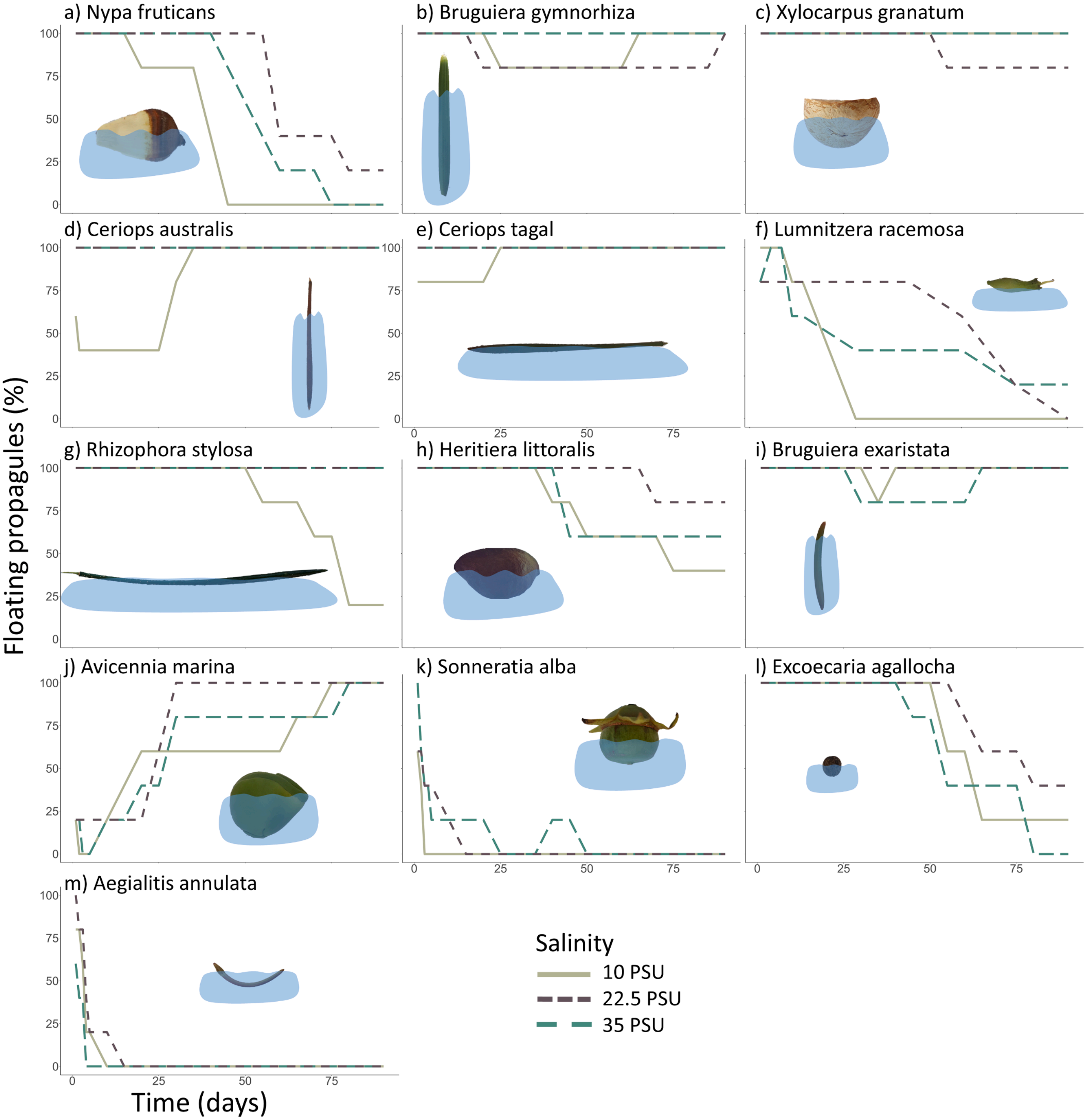

Fig. 2. Mean percentage of mangrove propagules that are floating at different salinities: 10 (solid light green line), 22.5 (dashed brown line) and 35 (dashed green line). Each treatment contains five replicates.

exposure above and below the waterline and root growth characteristics. Moreover, intraspecies differences were observed when propagules were subjected to varying salinity levels, with behaviours showing considerable variation over time. These results have significant implications for predicting mangrove dispersal and connectivity, as the duration of buoyancy and responses to salinity conditions were found to differ across species, demonstrating a higher complexity in biological parameters than what has been incorporated in biophysical models of mangrove dispersal. Additionally, we found that propagule exposure above and below the water surface also varies among species and salinity levels. Therefore, these factors must also be considered in modelling, as they impact aspects such as windage and drift factor, thereby influencing dispersal dynamics.

The morphology and behaviour in the water column of the mangrove propagules varied notably among the 13 species assessed here. Some species, such as *B. gymnorhiza, X. granatum, C. australis, C. tagal, R. stylosa* and *B. exaristata*, remained buoyant throughout the 90-day experiment, indicating their potential for prolonged dispersal via currents, tides and winds. Others, like *N. fruticans, L. racemosa, H. littoralis* and *E. agallocha*, were also buoyant but for shorter durations. While it is true that some literature reports extensive floating periods for species like *H. littoralis* (Clarke et al., 2001), it is worth noting that *H. littoralis* was the only species collected from the soil surrounding the parental tree, so the exact duration of its buoyancy prior to collection is uncertain. There

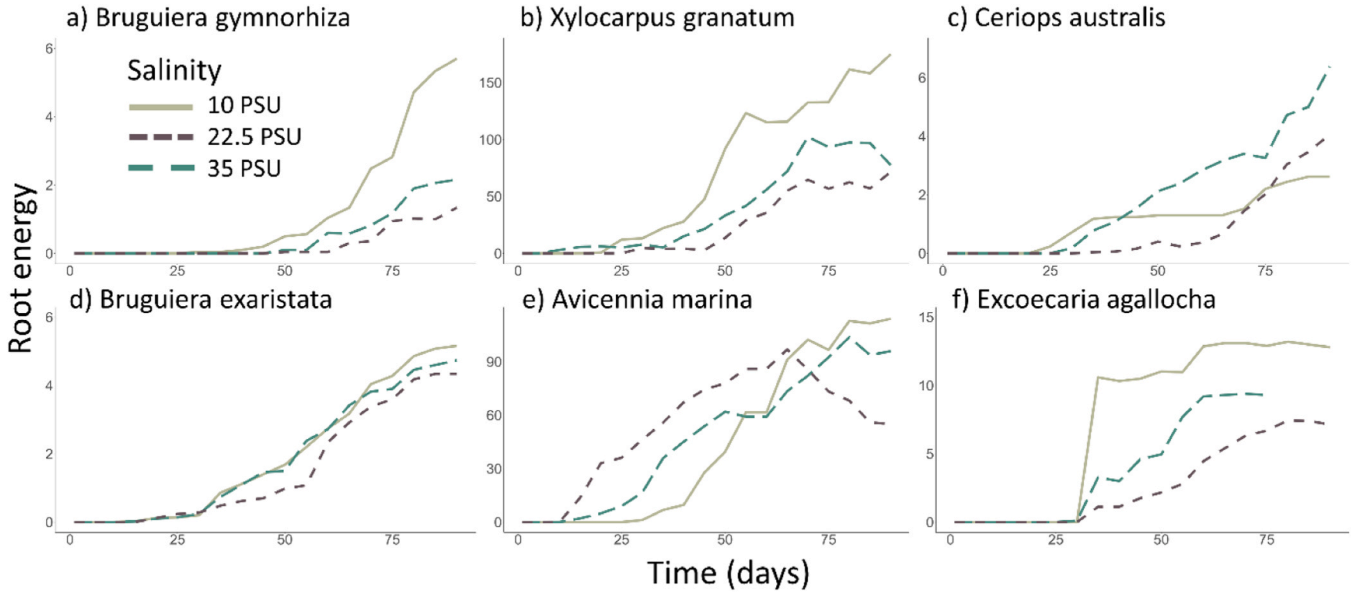

Fig. 3. Root energy representing the number of roots multiplied by the longest root for the six species that developed roots during the experiment. The lines represent the salinity concentration: 10 (solid light green line), 22.5 (dashed brown line) and 35 (dashed green line).

Table 3
Species-specific drift factor and windage values, detailing the salinity conditions, measurement times for areas above and below the water surface and corresponding values for drift factor and windage.

Species	Salinity	Time	Above surface	Below surface	Drift factor	Windage
Nypa fruticans	All	1	0.011	0.022	0.023547	0.024194
	All	30	0.007	0.027	0.022995	0.016788
	All	60	0.007	0.053	0.02118	0.012435
Bruguiera gymnorhiza	35	1	0.003	0.168	0.018075	0.004572
	35	30	0.012	0.182	0.01786	0.008601
	35	60	0.011	0.191	0.01773	0.008022
	22.5	1	0.004	0.013	0.024962	0.01898
	22.5	30	0.014	0.186	0.017801	0.009387
	22.5	60	0.021	0.19	0.017744	0.011375
	10	1	0.013	0.155	0.018292	0.009909
	10	30	0.016	0.164	0.018148	0.010535
	10	60	0.027	0.18	0.01789	0.013252
Xylocarpus granatum	All	1	0.004	0.019	0.023941	0.015699
	All	30	0.002	0.021	0.023672	0.010559
	All	60	0.002	0.025	0.023203	0.009678
Ceriops australis	All	All	0.001	0.119	0.019015	0.003143
Ceriops tagal	All	All	0.001	0.009	0.025952	0.011405
Lumnitzera racemosa	All	All	0.001	0.004	0.028135	0.017108
Rhizophora stylosa	All	All	0.003	0.011	0.025412	0.017869
Heritiera littoralis	All	All	0.01	0.022	0.023547	0.023068
Bruguiera exaristata	All	All	0.002	0.089	0.019785	0.005129
Avicennia marina	All	All	0.001	0.021	0.023672	0.007467
Sonneratia alba	35	All	0.003	0.031	0.022624	0.010644
	10	All	0.003	0.037	0.022184	0.008955
	22.5	All	0.001	0.036	0.022221	0.005703
Excoecaria agallocha	All	All	0.002	0.002	0.03	0.034216
Aegialitis annulata	All	All	1.00E−04	0.003	0.029	0.006354

was also a group of species, including *A. marina, S. alba* and *A. annulata*, which showed little potential for dispersal as they sank within the first days of the experiment. These findings align with those of Clarke et al. (2001), who conducted a similar experiment although over a shorter timeframe, obtaining similar patterns. Moreover, differences in buoyancy duration among species were reflected in their morphological traits, with longer and wider propagules generally remaining afloat longer, suggesting that these traits may influence dispersal potential.

Intraspecies variations in buoyancy were also apparent with changes in salinity concentration. Specifically, for *N. fruticans* and *E. agallocha*, notable differences were observed across different salinity treatments, indicating that salinity should be considered a crucial parameter when modelling the dispersal of these species. Additionally, buoyancy of all propagules that were tested changed throughout the experiment, including *N. fruticans, L. racemose* and *E. agallocha*. While previous mangrove dispersal models have considered the impact of time (Van der Stocken and Menemenlis, 2017), it was determined that the maximum floating period of 75 days post-detachment does not hold true universally across all species. This underscores the necessity of incorporating species-specific information when evaluating mangrove dispersal, given the observed variability among different species. It is worth noting that *N. fruticans* seeds in this study were relatively small compared to specimens from core populations, which have been reported to range between 20–30 cm (Numbere and Camilo, 2016), whereas our specimens

Table 4
Graph-level network measures of *Rhizophora stylosa* and *Bruguiera gymnorhiza* in the central Great Barrier Reef. For *R. stylosa*, only the drift factor was included, as the effect of windage was negligible.

Species	*Rhizophora stylosa*		*Bruguiera gymnorhiza*	
Measure	**Drift factor**	**No wind added**	**Drift factor and windage**	**No wind added**
Total edges	41018	28533	1348	1608
Network density	0.43	0.3	0.47	0.56
Network diameter	4	4	3	3
Connected components	3	3	3	3
Number of clusters (modularity)	11 (0.44)	23 (0.65)	5 (0.33)	8 (0.61)

measured a mean of 6.98 cm. It has been observed that larger seeds can float for extended periods and disperse over hundreds of kilometres (Robertson and Alongi, 1995). This suggests that the findings for *N. fruticans* in this experiment may represent the lower end of the species' dispersal capabilities.

In the case of *R. stylosa*, statistical analysis for buoyancy was not feasible due to insufficient variation for testing. However, notable differences were observed between the 10 PSU treatment and the other treatments. Propagules in the 10 PSU treatment sank while those exposed to higher salinity remained buoyant. These differences were likely attributable to the distinct collection sites. Propagules used in the 35 PSU and 22.5 PSU treatments were sourced from Ross River (Townsville), whereas those in the 10 PSU treatment were sourced from Lucinda. This sampling strategy was adopted because it was challenging to gather all necessary propagules from a single location. Additionally, propagules from the 10 PSU treatment were significantly smaller than those from the other sites, suggesting potential differences in developmental stage or environmental adaptation. Consequently, we cannot definitively conclude that the treatment itself influences the buoyancy of *R. stylosa*. It is plausible that variability in species buoyancy could also be linked to the geographical origin of the propagule. Propagule traits such as buoyancy, size and establishment time can vary and are often shaped by the typical position of the adult trees within the intertidal zone, with landward species generally producing smaller propagules that require longer periods free from inundation to establish (Rabinowitz, 1978). This pattern is concordant with our sampling, as propagules from Ross River were sourced from the low intertidal zone whereas those from Lucinda were collected from the mid intertidal zone. Propagules from Lucinda may have had different structural or physiological traits influencing their buoyancy, such as smaller size, reduced internal air cavities or higher density, linked to their intertidal origin or local environmental conditions. However, further investigations are needed to clarify the extent and causes of intraspecific variability in propagule traits across different locations.

A. marina, a pioneer species and the most widespread mangrove species (Osborne and Berjak, 1997), exhibits rapid sinking and early root development, which promotes quick local establishment while limiting long-distance dispersal. Its rapid sinking behaviour suggests a different dispersal strategy compared to other species. Consequently, the potential dispersal capabilities of *A. marina* may be overestimated in some biophysical models, which often emphasize buoyancy and long-distance dispersal. In previous studies, an early sink of *A. marina* seeds has also been observed (Clarke et al., 2001). Research on *A. marina* dispersal in southeastern Australia indicates that inter-population dispersal is infrequent due to the limited number of floating propagules, leading to restricted gene flow between populations (Clarke, 1993). However, it is important to note that while dispersal becomes less likely, it is still possible, as propagules that fail to settle may subsequently refloat, as it was seen in our experiments, and continue dispersing or they might be able to disperse under water. This aligns with observations of *A. marina* propagules found outside mangrove forests, which suggest that some propagules might not settle immediately and could disperse upon refloating (Minchinton, 2006).

As buoyancy alone does not solely determine propagule transport, we also examined propagule morphology, specifically assessing the proportion submerged and exposed. This information is essential for calculating windage (the effect of wind on the exposed portion of the propagule) and drift factor (the effect of wind-driven drift current on the submerged portion) (Van der Mheen et al., 2020). Our analysis revealed differences in salinity treatments for *B. gymnorhiza* and *S. alba*. Therefore, when applying windage and drift factor to these species in biophysical models, it is crucial to consider the salinity of the areas where the propagules are travelling. Furthermore, *N. fruticans, B. gymnorhiza* and *X. granatum* changed over time. Thus, the time propagules remain afloat should be considered when modelling the dispersal of these species as it has been previously described (Tonné et al., 2017). Moreover, in the case of *B. gymnorhiza*, it is also important to account for root and stem development, which occur around days 45 and 66 of the experiments, respectively, as they introduce additional drag. Given that the *B. gymnorhiza* propagules were mostly in a vertical position, root and stem lengths were incorporated into the drift factor and windage calculations to better represent the influence of wind-driven currents on their dispersal.

Testing drift factor and windage in *R. stylosa* and *B. gymnorhiza* showed that these physical drivers can substantially alter connectivity estimates, particularly for *R. stylosa*. The addition of drift factor in *R. stylosa* reduced the final distance travelled to almost half, nearly doubled the number of total connections, leading to higher network density and fewer clusters. This demonstrates that excluding this factor, which is essential for properly modelling the dynamics of *R. stylosa,* might result in underestimating connectivity, potentially leading to inaccurate modelling of the species and, consequently, misguided management decisions. A similar pattern was observed for *B. gymnorhiza,* where the final dispersal distance was reduced to less than half when drift factor and windage were included. However, the overall connectivity patterns of *B. gymnorhiza* were less affected by the inclusion of windage and drift factor than those of *R. stylosa*. Nevertheless, including these factors in the model, even for *B. gymnorhiza*, ensures a more robust and comprehensive understanding, minimizing the risk of potential oversights in the modelling process and produces ecologically realistic outcomes that can inform management. However, field validation, such as tracking analogous drifters or controlled propagule releases, remains necessary to confirm model accuracy.

Climate change is likely to affect the dispersal of mangrove propagules, primarily through alterations in salinity, currents and wind patterns (Alongi, 2015; Van der Stocken et al., 2022). Rising sea levels, changes in temperature, precipitation and evaporation rates are expected to alter coastal salinity regimes, potentially impacting the buoyancy and viability of mangrove propagules. For species like *N. fruticans*, *E. agallocha*, *L. racemosa*, *B. gymnorhiza* and *S. alba*, changes in salinity might have a greater impact, as these species show that their propagule buoyancy is influenced by salinity. Evidence indicates that warmer and less saline ocean conditions, attributed to increased freshwater input, could alter the dispersal paths of mangrove propagules and elevate sinking rates in less suitable offshore areas, potentially impacting the resilience of mangrove forests (Van der Stocken et al., 2022). For instance, *N. fruticans* propagules became less positively buoyant at lower salinity, suggesting that increased freshwater inputs under climate change could cause them to sink earlier, reducing their dispersal potential and limiting colonisation success in more distant habitats. In some areas the opposite might be true, higher salinity levels may enhance positive buoyancy, allowing propagules to travel greater distances; however, excessively high salinities could exceed the tolerance thresholds of certain species by affecting seed viability, metabolism or osmotic balance, leading to reduced dispersal success (Alongi, 2022). For example, while relatively salt-tolerant species such as *B. gymnorhiza* and *S. alba* can persist under high salinities, they still exhibit physiological stress when thresholds are exceeded, which may impair establishment (Feng et al., 2020; Zhu et al., 2012). More sensitive species, including *N. fruticans* and *E. agallocha*, are even more vulnerable, showing delayed germination, growth reductions or outright establishment failure under elevated salinity (Chen and Ye, 2014; Zaman et al., 2013). Understanding these thresholds is therefore critical for improving biophysical models of dispersal and for designing management strategies that anticipate how climate-driven changes in salinity regimes may constrain the resilience and future distribution of mangrove species.

In addition to changes in salinity, other variables such as changes in ocean currents, driven by shifting temperature gradients and altered wind patterns, can further transform dispersal dynamics. Enhanced or altered currents may facilitate longer dispersal distances, potentially aiding in the colonisation of new habitats or reduce dispersal distances and potentially hinder connectivity between mangrove populations, reducing genetic exchange and resilience (Alongi, 2015). Additionally, intensified wind patterns (Greene et al., 2010), including more frequent and severe storms (Brooks, 2013), could influence the propagules dispersal patterns. Increased wind strength might enhance or reduce dispersal distances for floating propagules but also poses the risk of depositing them in unsuitable environments, thereby reducing overall establishment success. Understanding these climate-induced changes is crucial for developing accurate predictive models and effective conservation strategies to maintain mangrove ecosystems in a rapidly changing world. Integrating species-specific responses to salinity, current alterations and wind patterns into these predictions will be essential for forecasting future dispersal patterns and ensuring the resilience of mangrove forests.

5. Conclusion

Our study highlights the variable influence of mangrove propagule traits on dispersal potential, shaped not only by buoyancy but also by morphological characteristics. Implementing drift factor and windage in biophysical models demonstrated the importance of incorporating these parameters to more realistically represent mangrove propagule dispersal. This approach enhances the accuracy of dispersal modelling, which is particularly critical in dynamic environments such as the Great Barrier Reef, but also relevant to more stable coastal systems. By refining and validating biophysical models, our findings provide valuable insights into mangrove population connectivity and strengthen the scientific basis for conservation and management.

Declaration of Competing Interest

The authors declare that they have no known competing financial interests or personal relationships that could have appeared to influence the work reported in this paper.

Acknowledgements

I would like to thank the Fisheries Planning & Assessment Unit of the Queensland Government for facilitating and granting the required permits to conduct this research (2212-127377 ADR-MP). Funding for this research was provided by James Cook University, Australian Government Research Training Program (RTP) Scholarship and the Australian Research Council Centre of Excellence for Coral Reef Studies (CE140100020). A.O-A was supported by Ramon y Cajal grant funded by the Ministry of Science and Innovation (RYC2023-043454-I). A.O-A research was conducted as part of the activities of the “Maria de Maeztu Centre of Excellence” accreditation to IMEDEA (CSIC-UIB) (CEX2021-001198), supported by the Spanish Government.

Appendix A. Supporting information

Supplementary data associated with this article can be found in the online version at doi:10.1016/j.rsma.2025.104528.

Data availability

The data supporting the findings of this study are available for access through the following link: https://doi.org/10.25903/0y2n-vv90

References

Alongi, D.M., 2015. The impact of climate change on mangrove forests. Curr. Clim. Change Rep. 1, 30–39.
Alongi, D.M., 2022. Climate change and mangroves. In Mangroves: Biodiversity, Livelihoods and Conservation. Springer, pp. 175–198.
Andutta, F.P., Ridd, P.V., Wolanski, E., 2011. Dynamics of hypersaline coastal waters in the great barrier reef. Estuar. Coast. Shelf Sci. 94 (4), 299–305.
Aziz, I., Khan, M.A., 2001. Effect of seawater on the growth, ion content and water potential of Rhizophora mucronata lam. J. Plant Res. 114 (3), 369.
Balbar, A.C., Metaxas, A., 2019. The current application of ecological connectivity in the design of marine protected areas. Glob. Ecol. Conserv. 17, e00569.
Breivik, Ø., Allen, A.A., Maisondieu, C., Roth, J.C., 2011. Wind-induced drift of objects at sea: the leeway field method. Appl. Ocean Res. 33 (2), 100–109.
Brooks, H.E., 2013. Severe thunderstorms and climate change. Atmos. Res. 123, 129–138.
Bürkner, P.-C., 2017. Brms: an R package for Bayesian multilevel models using stan. J. Stat. Softw. 80, 1–28.
Chamberlain, D., Phinn, S., Possingham, H., 2020. Remote sensing of mangroves and estuarine communities in central Queensland, Australia. Remote Sens. 12 (1), 197.
Chen, Y., Ye, Y., 2014. Effects of salinity and nutrient addition on mangrove excoecaria agallocha. PLoS One 9 (4), e93337.
Clarke, P.J., 1993. Dispersal of grey mangrove (Avicennia marina) propagules in southeastern Australia. Aquat. Bot. 45 (2-3), 195–204.
Clarke, P.J., Kerrigan, R.A., Westphal, C.J., 2001. Dispersal potential and early growth in 14 tropical mangroves: do early life history traits correlate with patterns of adult distribution? J. Ecol. 648–659.
Cowen, R.K., Gawarkiewicz, G., Pineda, J., Thorrold, S.R., Werner, F.E., 2007. Population connectivity in marine systems an overview. Oceanography 20 (3), 14–21.
Di Nitto, D., Erftemeijer, P., Van Beek, J., Dahdouh-Guebas, F., Higazi, L., Quisthoudt, K., Jayatissa, L., Koedam, N., 2013. Modelling drivers of mangrove propagule dispersal and restoration of abandoned shrimp farms. Biogeosciences 10 (7), 5095–5113.
Duke, N., 2006. *Australia's mangroves: the authoritative guide to Australia's mangrove plants*. MER.
Duke, N., Ball, M., Ellison, J., 1998. Factors influencing biodiversity and distributional gradients in mangroves. Glob. Ecol. Biogeogr. Lett. 7 (1), 27–47.
Duke, N., Lawn, P., Roelfsema, C., Phinn, S., Zahmel, K., Pedersen, D., Harris, C., Steggles, N., Tack, C., 2003. Assessing historical change in coastal environments. Port Curtis, Fitzroy River Estuary and Moreton Bay Regions.
Feng, X., Xu, S., Li, J., Yang, Y., Chen, Q., Lyu, H., Zhong, C., He, Z., Shi, S., 2020. Molecular adaptation to salinity fluctuation in tropical intertidal environments of a mangrove tree sonneratia alba. BMC Plant Biol. 20 (1), 178.
Goudkamp, K., Chin, A., 2006. Mangroves and saltmarshes.
Gouvêa, L.P., Fragkopoulou, E., Cavanaugh, K., Serrão, E.A., Araújo, M.B., Costello, M.J., Westergerling, E.T., Assis, J., 2023. Oceanographic connectivity explains the intra-specific diversity of mangrove forests at global scales. Proc. Natl. Acad. Sci. 120 (14), e2209637120.
Greene, S., Morrissey, M., Johnson, S.E., 2010. Wind climatology, climate change, and wind energy. Geogr. Compass 4 (11), 1592–1605.
Hamilton, J.F., Osman, R.W., Feller, I.C., 2017. Modeling local effects on propagule movement and the potential expansion of mangroves and associated fauna: testing in a sub-tropical lagoon. Hydrobiologia 803, 173–187.
Hamylton, S., Kelleway, J., Rogers, K., McLean, R., Tynan, Z.N., Repina, O., 2023. Mangrove expansion on the low wooded islands of the great barrier reef. Proc. R. Soc. B 290 (2010), 20231183.
Hartig, F., 2020. DHARMa: residual diagnostics for hierarchical (multi-level/mixed) regression models. R package version 0.3 3 (5).
Houston, W., 1999. Severe hail damage to mangroves at port curtis, Australia. Mangroves and Salt Marshes 3, 29–40.
Howe, H.F., Miriti, M.N., 2004. When seed dispersal matters. BioScience 54 (7), 651–660.
Howe, H.F., Smallwood, J., 1982. Ecology of seed dispersal. Annu. Rev. Ecol. Syst. 13 (1), 201–228.
Isobe, A., Hinata, H., Kako, S. i, Yoshioka, S., 2011. Formulation of leeway-drift velocities for sea-surface drifting-objects based on a wind-wave flume experiment. Interdisciplinary studies on environmental chemistry-marine environmental modeling and analysis. Terrapub., Tokyo 239–249.
Kathiresan, K., Bingham, B.L., 2001. Biology of mangroves and mangrove ecosystems.
McKillup, S., McKillup, R., 1997. An outbreak of the moth Achaea serva (Fabr.) on the mangrove Excoecaria agallocha (L.).

Minchinton, T.E., 2006. Consequences of pre-dispersal damage by insects for the dispersal and recruitment of mangroves. Oecologia 148 (1), 70–80.

NASA. (2025). *Salinity overview* Retrieved April 12, 2025 from ⟨https://salinity.oceansciences.org/overview-faqs.htm?utm_source=chatgpt.com⟩.

Ngeve, M.N., Van der Stocken, T., Menemenlis, D., Koedam, N., Triest, L., 2016. Contrasting effects of historical sea level rise and contemporary ocean currents on regional gene flow of rhizophora racemosa in eastern atlantic mangroves. PLoS One 11 (3), e0150950.

Numbere, A.O., Camilo, G.R., 2016. Reciprocal transplant of mangrove (Rhizophora racemosa) and nypa palm (Nypa fruticans) seedlings in soils with different levels of pollution in the Niger river delta, Nigeria. Glob. J. Environ. Res. 10 (1), 14–21.

Osborne, D.J., Berjak, P., 1997. The making of mangroves: the remarkable pioneering role played by seeds of Avicennia marina. Endeavour 21 (4), 143–147.

Proisy, C., Sidik, F., Prospéri, M.-J., Suhardjono, S., Tranchant, B., 2016. Connectivity of mangroves in the Indonesian archipelago through dispersal pathways of propagules using an ocean circulation model. In EcoSummit 2016 - Ecological Sustainability: Engineering Change. Montpellier, France: INRA, IRD.

R Code Team, 2019. R: A language and environment for statistical computing.

Rabinowitz, D., 1978. Dispersal properties of mangrove propagules. Biotropica 47–57.

Robertson, A.I., Alongi, D.M., 1995. Role of riverine mangrove forests in organic carbon export to the tropical coastal ocean: a preliminary mass balance for the Fly delta (Papua New Guinea). Geo-Mar. Lett. 15, 134–139.

Schupp, E.W., Jordano, P., Gómez, J.M., 2010. Seed dispersal effectiveness revisited: a conceptual review. New Phytol. 188 (2), 333–353.

Smith, S.M., Snedaker, S.C., 1995. Salinity responses in two populations of viviparous Rhizophora mangle L. seedlings. Biotropica 435–440.

Sousa, W.P., Kennedy, P.G., Mitchell, B.J., Ordóñez L, B.M., 2007. Supply-side ecology in mangroves: do propagule dispersal and seedling establishment explain forest structure? Ecol. Monogr. 77 (1), 53–76.

Steinberg, C., 2007. Impacts of climate change on the physical oceanography of the Great Barrier Reef.

Steinberg, R., van der Meer, M., Walker, E., Berumen, M.L., Hobbs, J.-P.A., van Herwerden, L., 2016. Genetic connectivity and self-replenishment of inshore and offshore populations of the endemic anemonefish, amphiprion latezonatus. Coral Reefs 35, 959–970.

Tomlinson, P.B., 2016. The botany of mangroves. Cambridge University Press.

Tomlinson, P.B., Cox, P.A., 2000. Systematic and functional anatomy of seedlings in mangrove rhizophoraceae: vivipary explained? Bot. J. Linn. Soc. 134 (1-2), 215–231.

Tonné, N., Beeckman, H., Robert, E.M., Koedam, N., 2017. Towards an unknown fate: the floating behaviour of recently abscised propagules from wide ranging rhizophoraceae mangrove species. Aquat. Bot. 140, 23–33.

Tsanis, I.K., 1989. Simulation of wind-induced water currents. J. Hydraul. Eng. 115 (8), 1113–1134.

Van der Mheen, M., Pattiaratchi, C., Cosoli, S., Wandres, M., 2020. Depth-dependent correction for wind-driven drift current in particle tracking applications. Front. Mar. Sci. 7, 305.

Van der Stocken, T., Carroll, D., Menemenlis, D., Simard, M., Koedam, N., 2019. Global-scale dispersal and connectivity in mangroves. Proc. Natl. Acad. Sci. 116 (3), 915–922.

Van der Stocken, T., Menemenlis, D., 2017. Modelling mangrove propagule dispersal trajectories using high-resolution estimates of ocean surface winds and currents. Biotropica 49 (4), 472–481.

Van der Stocken, T., Vanschoenwinkel, B., Carroll, D., Cavanaugh, K.C., Koedam, N., 2022. Mangrove dispersal disrupted by projected changes in global seawater density. Nat. Clim. Change 12 (7), 685–691.

Van der Stocken, T., Vanschoenwinkel, B., De Ryck, D.J., Bouma, T.J., Dahdouh-Guebas, F., Koedam, N., 2015. Interaction between water and wind as a driver of passive dispersal in mangroves. PLoS One 10 (3), e0121593.

Van der Stocken, T., Wee, A.K., De Ryck, D.J., Vanschoenwinkel, B., Friess, D.A., Dahdouh-Guebas, F., Simard, M., Koedam, N., Webb, E.L., 2019. A general framework for propagule dispersal in mangroves. Biol. Rev. 94 (4), 1547–1575.

Van Woesik, R., 1992. Ecology of coral assemblages on continental islands in the Southern section of the great barrier reef. Australia James Cook University.

Wu, J., 1983. Sea-surface drift currents induced by wind and waves. J. Phys. Oceanogr. 13 (8), 1441–1451.

Yao, Y., Vehtari, A., Simpson, D., Gelman, A., 2017. 1 When is leave-one-out cross validation appropriate?

Zainol, Z., Peris, A.D., Akhir, M.F., Rahim, N.H.A., Satyanarayana, B., Dahdouh-Guebas, F., 2022. Mangrove propagule dispersal in a shallow and narrow coastal lagoon: a simulation-based assessment of the setiu wetlands, Malaysia. Forests 13 (9), 1525.

Zaman, S., Raha, A.K., Mitra, A., 2013. Signals of salinity fluctuation in nypa fruticans seedling growth: a case study from lower gangetic plain. Indian J. For. 36 (3), 327–331.

Zhu, Z., Chen, J., Zheng, H.-L., 2012. Physiological and proteomic characterization of salt tolerance in a mangrove plant, Bruguiera gymnorrhiza (L.) lam. Tree Physiol. 32 (11), 1378–1388.